Journal of the Meteorological Society of Japan

EARLY ONLINE RELEASE

This is a PDF of a manuscript that has been peer-reviewed and accepted for publication. As the article has not yet been formatted, copy edited or proofread, the final published version may be different from the early online release.

This pre-publication manuscript may be downloaded, distributed and used under the provisions of the Creative Commons Attribution 4.0 International (CC BY 4.0) license. It may be cited using the DOI below.

The DOI for this manuscript is
DOI:10.2151/jmsj.2022-036
J-STAGE Advance published date: May 9th, 2022
The final manuscript after publication will replace the preliminary version at the above DOI once it is available.

Stratospheric Polar Vortex Revisited: New Diagnostic for the Vortex Breakup

Jihoon SEO

School of Earth and Environmental Sciences
Seoul National University, Seoul, Korea
and
Climate and Environmental Research Institute
Korea Institute of Science and Technology, Seoul, Korea

and

Wookap CHOI[1]

School of Earth and Environmental Sciences
Seoul National University, Seoul, Korea

November 1, 2021

----

1) Corresponding author: Wookap Choi, School of Earth and Environmental Sciences, Seoul National University, Seoul 08826, KOREA.
Email: wchoi@snu.ac.kr
Tel: +82-2-880-6711

Abstract

The stratospheric polar vortex and its breakup are important dynamical phenomena. In previous studies, three diagnostics for vortex breakup have been suggested by using the potential vorticity (PV) and zonal wind for the lower stratosphere. These three diagnostics, however, cannot be applied for the upper stratosphere, since the evolution of the polar vortex is more complicated and, therefore, it is more difficult to prescribe key parameters. Here we define the dates of the breakup and formation of the polar vortex by finding the maximum peaks in the averaged rates of change in the equivalent latitude, PV, and wind speed at the vortex edge. By applying our new definition to the ERA-Interim reanalysis data, the breakup and formation dates of the Arctic and Antarctic polar vortices for the whole stratosphere were obtained for 1979–2018. Our newly-defined vortex breakup date is compared with the date of the stratospheric final warming, which is defined as the timing of zonal mean westerlies changing to easterlies without recovering to a westerly exceeding the threshold westerly wind speed. To see if our definition is consistent with atmospheric transport near the vortex edge, the dates of the formation and breakup of the polar vortex are compared with the mixing ratios of long-lived trace species. It turns out that the newly defined dates well match the changes of concentrations of trace gases in the stratosphere for the winter of 1996–1997.

Considering all the above observations, our definition of the vortex formation and breakup appears to be applicable to the whole stratosphere.

Keywords polar vortex; vortex breakup; vortex formation; stratospheric final warming; potential vorticity

1. Introduction

The winter stratosphere is dominated by strong westerly wind and the polar vortex. The strong westerly wind during winter generates steep meridional gradients in potential vorticity (PV) and isolates an extremely cold air mass with high PV. This resulting polar vortex plays an important role not only in the large-scale circulation, distribution of trace gases, formation of the polar stratospheric cloud, and polar ozone depletion (Solomon 1999; Choi et al. 2002; Karpetchko et al. 2005) but also in the stratosphere-troposphere coupling on both intraseasonal and interannual timescales through the annular mode (Baldwin and Dunkerton 2001; Baldwin et al. 2003). Diagnostics of the polar vortex in previous studies have generally been based on two parameters, zonal wind and potential vorticity. The zonal mean zonal wind at certain latitudes and heights with a wind velocity criterion have been widely used to identify the onset of spring (Black et al. 2006; Black and McDaniel 2007; Hardiman et al. 2011; Hu and Ren 2014).

Defining the polar vortex by using the zonal winds is simple and easy to apply and provides useful information in the zonal mean sense. On the other hand, diagnosis using potential vorticity is more appropriate for quantifying the day-to-day variations in the polar vortex as well as its breakup events. Defining the edge of the vortex and its breakup is a useful diagnostic although it is somewhat subjective. Previously, three diagnostics for the polar vortex breakup have been discussed by Waugh et al. (1999) in detail. Following their notation, these are "PV area", "PV and U", and "U area". For future purposes, they are briefly summarized here:

(1) In the "PV area" method, the vortex breakup is defined when the area within a specific PV isoline, which represents the boundary of the polar vortex, becomes less than a minimum area (Manney et al. 1994; Waugh and Randel 1999). Waugh and Randel (1999) used the average PV at the daily boundary of the polar vortex for wintertime (December to February; DJF) for this specific PV value, and used the 80°-latitude circle for the minimum area.

(2) In the "PV and U" method suggested by Nash et al. (1996), the edge of the vortex is found using the maximum PV gradient constrained by strong nearby zonal wind, and the vortex breakup is defined to be when the average wind speed along the vortex edge becomes smaller than a critical value. Nash et al. (1996) used the criterion of 15.2 m s^{-1} for the breakup dates at 450 K.

(3) In the "U area" method by Waugh et al. (1999), the vortex breakup is defined to occur when the total area within which the zonal wind exceeds a specific value falls below a minimum value. Waugh et al. (1999) used 25 m s^{-1} as the criterion, and the region within the 75°-latitude circle as the minimum area.

All three methods require parameters to be prescribed and prescribing the necessary parameter values is relatively easy in the lower stratosphere, as shown in Section 3.1. In the upper stratosphere, however, it is hard to choose the right values for these parameters, and this is why an exact breakup date is not available for the upper stratospheric polar vortex. Dynamical features in the upper stratosphere are usually more complicated than those in the lower stratosphere. One reason is mid-winter sudden stratospheric warming (SSW); following SSWs, recovery of the westerly jet varies year-to-year. Thus, determining the criteria for the upper stratospheric vortex breakup is not easy compared to that for the lower stratospheric vortex.

Another important dynamical phenomenon in the stratosphere is the stratospheric final warming (SFW). Following Andrews et al. (1987), the SFW is the event that is followed not by a reversion of stratospheric conditions to the usual winter pattern but by a transition to the summer structure of warm temperatures and easterly winds. At the time of the SFW, which is often accompanied by the abrupt breaking of the polar vortex, the zonal wind reverses from a westerly to easterly wind. Similar to the SSWs, SFW events also affect the tropospheric circulation by rapid deceleration of the high-latitude circumpolar westerlies in both the stratosphere and troposphere (Black et al. 2006; Black and McDaniel 2007). In several studies SFWs are regarded as the same as the breakup of polar vortices (Black et al. 2006; Black and McDaniel 2007; Hardiman et al. 2011). The date of the SFW is a significant factor in understanding interannual and decadal variability, and thus has been extensively studied. SFWs are usually defined at the time when zonal mean zonal wind at a specific altitude and latitude fall below zero without returning to a threshold value until the subsequent autumn. The reason for the threshold value is that the zonal wind sometimes recovers from zero wind to a certain extent after a mid-winter SSW before it completely falls below zero. The date of the SFW can be sensitive to the choice of the threshold value (Fig. 12).

In this study, we suggest a method for defining the date of the breakup and formation of the polar vortex. This method does not require prescribing parameters and can be used in the upper stratosphere as well as in the lower stratosphere. The breakup dates obtained by this method are compared with SFW dates.

The boundary of the strong polar vortex plays the role of a transport barrier (Hartmann et al. 1989; Schoeberl et al. 1992) and, hence, the concentrations of trace species that are rich in the subtropics have large differences across the vortex boundary. As shown in Choi et al. (2002), concentration of long-lived chemical species is a good indicator of the evolution of the polar vortex. By observing tracer concentrations, we were able to evaluate the usefulness of our new definition of vortex formation and breakup. The formation and breakup dates of the polar vortices are compared to the mixing ratios of methane (CH_4), nitrous oxide (N_2O), water vapor (H_2O), and ozone (O_3) observed by satellite instruments.

In section 2, the data and analysis techniques used in this study are described. Section 3 presents different characteristics of the upper and lower stratospheric polar vortices and suggests an alternative diagnostic for the vortex breakup. The newly defined formation and breakup dates of the polar vortex are compared with satellite tracer measurement data in section 4. Finally, the key findings are summarized in section 5.

2. Data

Air temperature and wind data for the period 1979–2018 were obtained from the European Center for Medium-Range Weather Forecasts Re-Analysis Interim (ERA-Interim; Dee et al. 2011). The data are defined on 37 pressure levels from the surface to 1 hPa at 1.5° horizontal resolution. The number of temperature observations is limited in the upper stratosphere due to the height limitations of the radiosonde, which induces bias in the reanalysis dataset (Marlton et al., 2021). A lack of reliability of the upper stratospheric dataset can also be another reason for difficulty in the breakup diagnosis at this level. The isobaric variables are interpolated onto 22 isentropic levels from 380 K (~15 km altitude) to 1260 K (~41 km altitude) with 1.2-km vertical spacing before calculating the isentropic PV. Since the isentropic PV increases exponentially with height, we produced the modified PV (hereafter MPV) following Lait (1994) by multiplying a scaling factor of $(\theta/\theta_0)^{-9/2}$, where θ_0 is the reference potential temperature of 420 K. The unit for MPV is the potential vorticity unit (PVU), where 1 PVU is 10^{-6} K m^2 kg^{-1} s^{-1}. The two-dimensional spatial distribution of PV can be simplified by conversion into a monotonic one-dimensional function of the area enclosed by each MPV isoline or equivalent latitude (EL), that is, a latitude equivalent to the area within the PV isoline (Butchart and Remsberg 1986).

For the data of stratospheric trace gases, mixing ratios of methane (CH_4), nitrous oxide (N_2O), water vapor (H_2O) and ozone (O_3) from the Improved Limb Atmospheric Spectrometer (ILAS) were used, which is an instrument onboard the Advanced Earth

Observing Satellite (ADEOS) (Sasano et al. 1999; Yokota et al. 2002). ILAS uses the solar occultation method and observes only the high latitude regions. Although the solar occultation measurements have disadvantages of low sampling frequency and limited latitudinal coverage compared to the limb emission sounding, they give the most accurate concentration data. During the 8 months of operation from November 1996 through June 1997, ILAS observations covered the Northern (57°N–72°N) and Southern (64°S–89°S) Hemisphere high latitudes. During any day, observations took place up to 14 times following the latitude circle.

In addition to the above data, we used the ozone mixing ratio from the Polar Ozone and Aerosol Measurement (POAM) II and POAM III (Glaccum et al. 1996; Lucke et al. 1999). POAM II and III are on-board the Satellite Pour l'Observation de la Terre (SPOT) 3 and SPOT 4 satellites, respectively. POAM II and III, which also uses the solar occultation technique, covers the periods from November 1993 to November 1996 and from April 1998 to December 2005, respectively. The mixing ratio of ozone was used since long-lived chemical species such as CH_4 and N_2O were not observed by POAM II and III. Ozone was observed up to 14 times in a day following the latitude bands of 54°N–71°N and 63°S–88°S.

3. Diagnostics for the Breakup of the Polar Vortex

3.1 Vortex Evolution in the Lower Stratosphere

Before defining the vortex breakup in the upper stratosphere, we show the evolution of a lower stratospheric vortex to reveal the characteristic features and how they differ from those in an upper stratospheric vortex. The evolution of the polar vortex represented by MPV is shown in Fig. 1 on the 450 K (~17 km) isentropic surface. The meridional gradient of MPV is over EL, and average wind speed along the MPV isolines are also shown. The year 1996–1997 is chosen, when ILAS data are available, and we can compare the vortex evolution with tracer concentrations later. The variables shown here are smoothed three times by 1-2-1 smoothing (3-point moving average by using 0.25:0.5:0.25 weighting) in EL and by a 5-day running mean in time. The location of the vortex edge is defined by the maximum of the average wind multiplied by the meridional gradient of the MPV in EL. From January through April 1997 the maximum MPV gradient is located near 65°N and is in good agreement with the maximum wind speed. The edge of the polar vortex is also located near the maximum MPV gradient during the same time period. In May, the polar vortex decays rapidly.

To observe the characteristic features of the vortex more clearly, three days are selected in Fig. 1, denoted by A, B, and C. Those days represent the mature vortex (10 March), and before (10 May) and after (20 May) the breakup of the polar vortex, respectively. In Fig. 2, the MPV gradient and the wind speed over EL, as well as the isentropic distribution of MPV are shown on those days. In the mature stage of the polar vortex on 10 March, the edge of the polar vortex with 20.1 PVU (Fig. 1a) corresponds to distinct peaks in both MPV gradient and wind speed at the EL of 65°N (Fig. 2a). The edge is also clearly discernible by the color contrast in the MPV distribution in Fig. 2d. As the season progresses toward summer, the polar vortex weakens, and both the maximum MPV value and the area of the polar vortex decrease. On 10 May, the edge of the vortex with 17.4 PVU (Fig. 1) at 69°N has a much smaller MPV gradient and wind speed, and the vortex has broken into two parts (Fig. 2e). On 20 May, the peaks in both MPV gradient and wind speed are not found any more (Fig. 2c), and the vortex shape does not appear in the isentropic distribution (Fig. 2f). Therefore, the polar vortex must have broken up sometime in the period 10–20 May 1997.

To determine the exact vortex breakup date, three diagnostics, which are summarized by Waugh et al. (1999), have been used. All of them can be easily applied to the above case since the vortex evolution is simple. In Fig. 3, the three methods are applied to obtain the date of the vortex breakup. To apply the "PV area" method (Fig. 3a) the value of MPV is needed to represent the location of the edge, and the average MPV during DJF is used following Waugh and Randel (1999). As shown in Figs. 1 and 3a, MPV has some small variability during DJF at the vortex edge. Since the MPV value at the vortex edge does not change much, using the average winter value of 18.6 PVU seems reasonable. By using this value and the MPV at 80°N in EL, we determined the vortex breakup date to be 17 May, 1997.

In the "PV and U" method (Fig. 3b), we define the date of the vortex breakdown as the date when the maximum wind speed averaged along the MPV isolines falls below 15.2 m

s^{-1}, following Nash et al. (1996). The choice of the value 15.2 m s^{-1} in the lower stratosphere is somewhat arbitrary, but it looks to be applicable for the case in Fig. 3b. This method determines the date of the polar vortex breakup to be 13 May, 1997. Using the "U area" method in Fig. 3c, when the zonal wind speed at 75°N becomes smaller than a threshold value of 25 m s^{-1}, following Waugh et al. (1999), the polar vortex breakup date is determined to be 3 May, 1997. The dates of the 1996–1997 Northern Hemisphere (NH) polar vortex breakup at 450 K defined by three different methods are dependent on the choice of parameters. Although choosing these parameters is subjective, determining the vortex dates can be done after proper "tuning" of the parameters, as suggested by Waugh et al. (1999), particularly for the study of the interannual variations.

3.2 Vortex Evolution in the Upper Stratosphere

To see if the same approaches used in section 3.1 are applicable for determining the vortex breakup in the upper stratosphere, we analyzed a case for the upper stratospheric vortex. Figure 4 exhibits the evolution of the polar vortex within the same time period at 1260 K (~41 km). In contrast to the lower stratosphere, MPV isolines show more complex behavior, and this is due to the occurrence of mid-winter breakup of the polar vortex.

To use the "PV area" method, we need the MPV value representing the vortex edge. In this case, the DJF mean of the MPV at the daily vortex edge is 18.9 PVU (green line in Fig. 4a) and appears to represent the seasonal vortex boundary only until late February. The vortex breakup date obtained using 18.9 PVU is 5 April. Following this, another vortex, which formed in late February is still present (Fig. 4a) near 60°N in EL. In contrast to the lower stratosphere (Fig. 1), the upper stratosphere in 1997 experiences significant variability in MPV during winter and, thus, defining the vortex edge by the winter-average MPV is not plausible. If we considered a different MPV value instead of the DJF mean, it could be found using Fig. 4b. From 18 February through 10 April during the late stages of the vortex, the value of MPV does not change much at the edge, and its average for the 52-day period is 14.4 PVU. If we choose this value to define the vortex edge, then the vortex breakup date would be diagnosed as 28 April. Without selecting the appropriate MPV value, which is applicable to the upper stratosphere each year, we are not able to use the "PV area" method for the whole stratosphere.

To use the other two methods, "PV and U" and "U area", the wind speed criteria require the threshold value. Since the wind speed increases with height in the winter stratosphere, it is difficult to choose a threshold value applicable to the whole stratosphere. For these reasons, all three diagnostic methods defined in section 1 are unsuitable for defining the vortex breakup date in the upper stratosphere.

To observe the evolution of the upper-stratospheric vortex more closely, 4 days are selected to represent the important phases: 15 January, 10 February, 25 March, and 15 April, marked by red lines A–D, respectively, in Fig. 4a. Their MPV distributions and their gradients are exhibited in Fig. 5. The edge of the vortex at 59°N on 15 January (Figs. 5a and 5e) rapidly moves poleward and is located at 79°N on 10 February (Figs. 5b and 5f). There is another maximum in the MPV gradient at 50°N (Fig. 5b), and it moves poleward (Fig. 4a). This second maximum in Fig. 5b is not a vortex edge by our definition at the present time, but it could grow to become a vortex edge. This second maximum also moved poleward and finally became an edge found at 61°N on 25 March (Figs. 5c and 5g). By observing the absence of the vortex on 15 April (Figs. 5d and 5h) we suggest that the vortex broke up between 25 March and 15 April. If this is indeed the case, the breakup date of 28 April estimated using the "PV area" method would be too late. The subtropical edge shown in Figs. 5d and 5h is discussed in the next section.

3.3 New Diagnostic for Vortex Breakup Date

Difficulties in the application of the diagnostics described in section 1 to the upper stratospheric vortex generally arise from the varying dynamical properties of the polar vortex with respect to altitude. To find an alternative diagnostic for vortex breakup regardless of the altitude, features common to the polar vortex in both the lower and upper stratosphere need to be found. In a similar sense, the features commonly observed during both the formation and breakup stages of the vortex should be considered. We have been concentrating on the mid-to-high latitudes, since our focus is on the breakup of the vortex. To see the vortex formation, its temporal evolution in the lower latitudes also needs be observed.

Figure 6 shows the characteristic features of the vortex evolution, as in Fig. 1 (same smoothing), but over the extended latitudinal range of 10°S–80°N in EL on the 1260 K isentropic surface. In addition to the vortex edge appearing in the polar region in winter, distinguishable edges are also seen in the subtropical region near 30°N in July 1996 and April-July 1997. These summertime edges are mainly determined by the maximum MPV gradient rather than strong zonal winds. In general, quasi-horizontal mixing by wave breaking in winter strengthens the horizontal PV gradients at both the poleward and the subtropical edges of the stirring zone (Polvani et al. 1995). The remnant of a wintertime subtropical edge could remain until summer (Nakamura and Ma 1997; Neu et al. 2003). For example, a minor edge exhibited by the MPV gradient at 28°N on 25 March (Figs. 5c and 5g) still remains on 15 April at 34°N (Figs. 5d and 5h), and it appears in Fig. 6 as a major edge after the polar vortex vanishes.

The EL of the daily vortex edge in Fig. 6 shifts rapidly between the low and high latitudes, and this is more clearly seen in Fig. 7a. The rapid shift from high to low latitudes in spring is associated with the vortex breakup, and the shift from low to high latitudes in autumn is associated with the vortex formation. Since the MPV and zonal wind speed at the polar vortex edge in Figs. 7b and 7c are significantly bigger than those at the tropical or subtropical edge, the MPV and wind speed at the edge in winter can be clearly distinguished from those in summer. Therefore, considering the parameters that are important for the existence of the polar vortex, such as high EL, large PV, and strong wind speed, the formation and breakup of the polar vortex could be characterized by the rapid increase and decrease of each variable at the edge, respectively. In other words, the formation and breakup of the polar vortex could be determined by detecting the peaks in the rate of temporal changes in EL, MPV, and wind speed at the edge. Therefore, we attempt to utilize the temporal changes of these three parameters at the edge to define the dates of the polar vortex formation and breakup.

In our calculations, the temporal change in the variables at the edge is obtained after using the 10-day running mean to reduce large day-to-day noise of each variable. The rate of change of each variable is normalized by its standard deviation for the entire period of data. Figure 7d shows the normalized rates of temporal changes of EL by the green line, MPV by the red line, and wind speed by the blue line, at the edge. The dates of positive and negative peaks of each variable are generally in good agreement with each other. In Fig. 7d, however, the opposite signs of peaks are observed between the wind speed and the other variables in midwinter. In January and February 1997, the sign of peak wind speed is opposite to those of EL and MPV. The reason is that the maximum wind speed appears in middle latitudes in contrast to MPV, which increases with the latitude. As shown in Fig. 6, wind speed decreases while the MPV increases during the poleward movement of the vortex edge in January, and that is the reason for the opposite signs of the variables in Fig. 7d. During the vortex formation (breakup), however, the wind speed increases (decreases) rapidly, and thus all three variables show the common sign of the peaks. Since the size of the peaks are different depending on the variable, we combine the three variables together to detect the meaningful peaks in the time series rather than considering them all individually. Therefore, we averaged the values from three lines to obtain the dates of the maximum peaks (black line).

The positive and negative maximum peaks of the black line appear on 22 September, 1996, and 7 April, 1997, and we define these as the formation and breakup of the polar vortex, respectively. Considering the observations in Fig. 5d, 7 April seems to be acceptable as a breakup date. We call this new method the “edge-change” method, and define the term "edge-change metric" as the values of the black line in Fig. 7d. There are also several minor peaks in the average change rate that are due to intraseasonal variability in the strength and area of the polar vortex, associated with the upward propagation and breaking of the planetary waves. However, these minor peaks generally appear in midwinter and are distinguishable from the maximum peaks related to the formation and breakup of the vortex.

Determining the dates of vortex formation and breakup by the "edge-change" method is possible for the lower stratosphere, where other diagnostics have been applied previously. Figure 8 shows a comparison of breakup dates of the NH polar vortices from 1979 to 2018, determined by the "edge-change" method defined in this study, and the "PV area", "PV and U", and "U area" methods on the 510 K (~21 km) isentropic level. The interannual variability in the breakup dates in Fig. 8 generally agrees well with Fig. 2 in Waugh et al. (1999), and with Fig. 8 in Waugh and Polvani (2010), who showed the breakup dates of the NH polar vortices at 500 K. In addition, there are generally good agreements between the breakup dates from the "edge-change" method and the dates from the other three methods. Therefore, the "edge-change" method may be considered as giving similar results to those obtained by other methods, for the lower stratosphere.

Note that there are some cases showing significant differences between the breakup dates. Years of 2009 and 2013 are among them (red diamonds in Fig. 8), and the major SSWs occurred in these two years (Harada et al. 2010; Nath et al. 2016). In these years, observing the evolution of the MPV distribution and the vortex edge such as in Fig. 9 would be useful to find the appropriate breakup date. The maximum negative peaks in the "edge-change" metric are found on 16 February in 2009 and 31 January in 2012, which are obviously associated with the SSW. In Figs. S3 and S4, the polar vortex, which is split and weakened after the day of maximum negative "edge-change" metric, recovers again and remains until the second negative peak days of 26 April 2009 and 3 May 2013. Therefore, choosing the next dates of the maximum rate of change, 26 April in 2009 and 3 May in 2012, would be more appropriate for determining the breakup dates, and those two dates are shown in Fig. 8. To identify the NH vortex breakup day in an objective manner, we define the vortex breakup day as the date of the negative peak "edge-change" metric after March 1 based on the observations in Figs. 8 and 9. If there were no vortex edge after March 1, the last day of the negative peak "edge-change" metric before March 1 would have been defined as the breakup date.

An advantage of the "edge-change" method is that a consistent determination can be made for the formation and breakup dates of the polar vortex regardless of altitude. Figure 10 shows vertical profiles of the formation and breakup dates from 430 K (~16 km) to 1260 K (~41 km) of the NH and Southern Hemisphere (SH) polar vortex for the period 1979–2018. In general, the formation and breakup of the polar vortex occur earlier in the upper stratosphere and later in the lower stratosphere. This downward propagation of formation- and breakup-timing of the polar vortex has been reported in several studies (Manney and Sabutis 2000; Choi et al. 2002; Hardiman et al. 2011). The formation and breakup dates show different characteristics in each hemisphere. In the NH, the polar vortex first formed late in September at 1260 K, and the formation took about 116 days until it arrived mid-January at 430 K (Fig. 10a). The breakup of the NH polar vortex, however, took only approximately 35 days on average with large year-to-year variability in its vertical profiles (Fig. 10b). In the SH, the vortex formation from 1260 K to 430 K took 92 days on average between early March and mid-April, which is much shorter than in the NH (Fig. 10c). The breakup of the SH polar vortex (Fig. 10d) took about 67 days covering the same altitude range. This is longer than for the NH vortex breakup, and it also shows less interannual variability.

Figure 11 shows the time series of the polar vortex breakup dates determined by the “edge-change” method for two isentropic levels of 1260 K and 510 K for 1979–2018. In SH, linear trends are drawn before and after 2000 in Figs. 11b and 11d. The year 2000 is subjectively chosen. Vortex breakup in SH has been delaying in the lower stratosphere until around 2000, with a statistically significant linear trend at a 95% confidence level (p=0.018). After 2000 a small and statistically insignificant trend is exhibited in the vortex breakup date in Fig. 11d. The trends before and after 2000 may be associated with the depletion and recovery of the Antarctic ozone layer. In their Fig. 6, Langematz and Kunze (2006) showed a significant change in the trend of the spring changeover around 2000 in the SH. Zambri et al. (2021) reported that the Antarctic column ozone in November decreased during 1979–2001 (−47 DU decade^{-1}), but started to recover after 2001 (+24 DU decade^{-1}). Trend in the upper stratosphere is of opposite sign until around 2000, although it is statistically insignificant. There is no significant decadal trend in the NH vortex breakup dates.

3.4 Comparison of the Vortex Breakup with the SFW

Vortex breakup dates constitute a good diagnostic for studying interannual climate change, specifically, by analyzing the vortex evolution.

Another diagnostic for understanding the vortex evolution is the SFW. As in Introduction, the SFW is defined as the event followed by the transition from the usual winter to the summer stratospheric conditions (Andrews et al., 1987). The date of the SFW is easier to define than the breakup date, particularly in the upper stratosphere since only the zonal wind is used for defining the SFW. The vortex breakup dates defined in this study are shown in Fig. 12 along with the SFW dates, for 430 K to 1260 K. The date of the SFW is defined when the zonal-mean zonal wind falls below zero without returning above a threshold value until the subsequent autumn (Black et al. 2006). The threshold value must be prescribed, and Black et al. (2006) used 5 m s^{-1} at 50 hPa, and 10 m s^{-1} at 10 hPa. The zonal-mean zonal wind in Fig. 12 was smoothed using a 5-day running mean and averaged between 60°N–80°N.

We obtained the date of the SFW in the NH by using both the 5 m s^{-1} and 10 m s^{-1} threshold and shown in Fig. 12 for the period of 1992–2005. This period is identical to that shown in Figs. 15 and 16. See Figs. S1 and S2 for the rest of the data period. In Fig. 12, the SFW date by the 10 m s^{-1} threshold is represented by green diamond. The SFW date by the 5 m s^{-1} threshold is shown by yellow square only when the two SFW dates by the different thresholds are not identical. The date of the SFW is generally not very sensitive to the choice of the threshold value. When the SSW occurs, however, determining the SFW date can be significantly affected by the threshold value, e.g., for the case in 2001 and 2002 (See the list of the SSW events in Table 1 of Choi et al. 2019). In 2001 (Fig. 12j), on the 760 K surface, the estimated SFW date with the 10 m s^{-1} threshold is found to be 2 February, while the date would be 13 May if the threshold were 5 m s^{-1}. In 1999 and 2000 (Figs. 12h and 12i), the SFW date in the upper stratosphere is also sensitive to the choice of the threshold value.

4. Vortex Breakup Diagnosed with Changes in Tracer Distribution

Mixing ratios of long-lived tracers such as CH_4 and N_2O exhibit large differences before and after the vortex breakup (Choi et al. 2002), associated with irreversible mixing. Thus, our definition of the vortex breakup date can be evaluated using the evolution of the tracer concentrations. Fig. 13 shows the temporal evolution of CH_4 and O_3 mixing ratios observed by ILAS from 1 November 1996 through 30 June 1997 on the isentropic levels of 1260 K (~41 km), 800 K (~32 km), and 450 K (~17 km). High and low mixing ratios of CH_4 and O_3, represented by the color scale, exhibit the boundary of the polar vortex fairly well. In the lower stratosphere (at the 450 K level) significantly high mixing ratios are observed inside the vortex, and this is due to a weaker transport barrier than in the mid-stratosphere (800 K), as shown by Haynes and Shuckburgh (2000) using the effective diffusivity. The EL at which the mixing-ratio discontinuity appears generally agrees well with the vortex edge defined dynamically, even in the upper stratosphere. These distinctive differences in CH_4 and O_3 across the edge of the polar vortex do not appear after the breakup date, and the tracers have a uniformly well-mixed distribution from low to high latitudes.

Significant discontinuities of tracer concentrations across the vortex edge in EL (Fig. 13) can also be observed on the same latitude circle (Fig. 2 from Choi et al. 2002), which show large and small mixing ratios outside and inside the vortex, respectively. After vortex breakup, the tracer mixing ratio has relatively similar values following the latitude circle due to the absence of the vortex edge. Thus, another diagnostic for the vortex breakup might be the standard deviation of the tracer mixing ratio following the latitude circle, which decreases significantly afterwards. The date of the vortex breakup at each level is shown by red dots in Fig. 14, along with the standard deviations of CH_4, N_2O, H_2O, and O_3 mixing ratios. The breakup dates distinguish between the high and low standard deviations before and after, and this implies the mixing of air from inside and outside the vortex and subsequent disappearance of the vortex edge.

To observe vortex formations and breakups over a longer time period, the O_3 mixing ratio was obtained from POAM II and POAM III in addition to the ILAS data. The standard deviation of the O_3 mixing ratio from the combined POAM II, ILAS, and POAM III data are shown in order, in Figs. 15 and 16. The formation and breakup dates are generally in good agreement with the high and low daily maximum MPV as well as the high and low zonal standard deviation of O_3, respectively. In Fig. 12j, our estimation includes an exceptionally early breakup date in February 2001 in the lower stratosphere. When comparing with the O_3 standard deviation in Fig. 15, the early vortex breakup date appears to be consistent with the evolution of O_3 concentration. Considering the observed features of tracer concentrations discussed in this section, the definition of vortex formation and breakup using the "edge-change" method seems to be well supported by their distribution and evolution.

5. Summary

Vortex breakup in the stratosphere is an important dynamical phenomenon, and determining its date has significant potential for understanding climate change. In previous studies the date of vortex breakup has been diagnosed using three methods: "PV area", "PV and U", and "U area". All of these methods were used successfully for the lower stratosphere near the 450–500 K isentropic levels following some "tuning" of key parameters (Waugh et al. 1999). In the upper stratosphere, however, subjectively choosing the parameters is more difficult due to the complex features in the vortex evolution.

This study has focused on the temporal change of the EL, MPV, and zonal wind at the vortex edge, which have been observed to change significantly at the time of vortex breakup and formation (Fig. 7). Based on these observations, the dates of the formation and breakup of the polar vortex are defined by finding the maximum peaks in the averaged rates of change in EL, MPV, and wind speed at the vortex edge. We applied the “edge-change” method to 22 isentropic levels in both the NH and SH from 380 K (~ 15 km) to 1260 K (~41 km) for the period 1979–2018, using the ERA-Interim reanalysis data. The onset and breakup dates of the polar vortices generally start from the upper stratosphere and propagate downwards to the lower stratosphere. For the lower stratosphere, the “edge-change” method shows similar results to those obtained by the other three diagnostic methods from previous studies.

The SFW is another diagnostic for the evolution of the stratospheric vortex, and we compared the SFW dates with our newly-defined vortex breakup dates. The dates of the

SFW are close in both the lower and upper stratosphere, while the vortex breakup dates mostly appear later in the lower stratosphere. Usually the SFW date is not very sensitive to the choice of threshold value. In some cases, however, the SFW date can be different by up to two months when the midwinter SSW occurs. Therefore, the vortex breakup date seems to be dynamically consistent throughout the stratosphere and could be more useful for observing interannual changes in the polar vortex.

The polar vortex plays an important role as a transport barrier for stratospheric tracers. Thus, analysing tracer concentrations along with the evolution of the vortex is useful in understanding the transport of tracers in the stratosphere. Comparison between the dates of polar vortex breakup defined in this study and the evolution of the CH_4 and O_3 mixing ratios show that discontinuities of tracer concentrations through the EL became much smaller just after the breakup date. Furthermore, zonal standard deviation of the tracer mixing ratio following the latitude circle decreases significantly after the dynamically obtained vortex breakup date. These observations apply to both the upper and lower stratosphere, and in both the NH and SH. Using these observations, determining the date of the vortex breakup by the "edge-change" method seems to be supported by transport of tracers. Therefore, our definition of the breakup date based on the “edge-change” could be an acceptable diagnostic for the polar vortex in both the lower and upper stratosphere.

Data Availability Statement

The ERA-Interim data can be accessed via the European Centre for Medium-Range Weather Forecasts (ECMWF) data server (http://apps.ecmwf.int/datasets/%20data/interim-full-daily/). The ILAS data were processed at and provided by the ILAS Data Handling Facility, National Institute for Environmental Studies (NIES) (http://www.nies.go.jp/link/archivs/ILAS-e.html). The POAM II / III data were provided by the Atmospheric Science Data Center at NASA Langley Research Center (https://asdc.larc.nasa.gov/project/POAM).

Supplement

Supplements 1 and 2 show the same as Fig. 12, but for the periods of 1979–1991 and 2006–2018, respectively. Supplements 3 and 4 show the same as Fig. 2, but for the years of 2009 and 2013, respectively.

Acknowledgments

We are grateful to Prof. Kwang-Y. Kim for his help on the manuscript. This work was supported by the National Research Foundation of Korea (2018R1A2B6003197).

References

Andrews, D. G., J. R. Holton, and C. B. Leovy, 1987: *Middle Atmosphere Dynamics.*

International Geophysics, **40***.* Elsevier, New York, 489 pp.

Baldwin, M. P., and T. J. Dunkerton, 2001: Stratospheric harbingers of anomalous weather regimes. *Science*, **294**, 581–584, doi:10.1126/science.1063315.

Baldwin, M. P., D. B. Stephenson, D. W. J. Thompson, T. J. Dunkerton, A. J. Charlton, and A. O'Neill, 2003: Stratospheric memory and skill of extended-range weather forecasts. *Science*, **301**, 636–640, doi:10.1126/science.1087143.

Black, R. X., B. A. McDaniel, and W. A. Robinson, 2006: Stratosphere-troposphere coupling during spring onset. *J. Climate*, **19**, 4891–4901, doi:10.1175/JCLI3907.1.

Black, R. X., and B. A. McDaniel, 2007: The dynamics of Northern Hemisphere stratospheric final warming events. *J. Atmos. Sci.*, **64**, 2932–2946, doi:10.1175/JAS3981.1.

Butchart, N., and E. E. Remsberg, 1986: The area of the stratospheric polar vortex as a diagnostic for tracer transport on an isentropic surface. *J. Atmos. Sci.*, **43**, 1319–1339, doi:10.1175/1520-0469(1986)043<1319:TAOTSP>2.0.CO;2.

Choi, H., B.-M. Kim, and W. Choi, 2019: Type classification of sudden stratospheric warming based on pre- and postwarming periods. *J. Climate*, **32**, 2349–2367, doi:10.1175/JCLI-D-18-0223.1.

Choi, W., S. Kim, W. B. Grant, M. Shiotani, Y. Sasano, and M. R. Schoeberl, 2002: Transport of methane in the stratosphere associated with the breakdown of the Antarctic polar vortex. *J. Geophys. Res.*, **107**, 8209, doi:10.1029/2001JD000644.

Dee, D. P., S. M. Uppala, A. J. Simmons, P. Berrisford, P. Poli, S. Kobayashi, U. Andrae, M. A. Balmaseda, G. Balsamo, P. Bauer, P. Bechtold, A. C. M. Beljaars, L. van de Berg, J. Bidlot, N. Bormann, C. Delsol, R. Dragani, M. Fuentes, A. J. Geer, L. Haimberger, S. B. Healy, H. Hersbach, E. V. Hólm, L. Isaksen, P. Kållberg, M. Köhler, M. Matricardi, A. P. McNally, B. M. Monge-Sanz, J.-J. Morcrette, B.-K. Park, C. Peubey, P. de Rosnay, C. Tavolato, J.-N. Thépaut, and F. Vitart, 2011: The ERA-Interim reanalysis: configuration and performance of the data assimilation system. *Q. J. R. Meteorol. Soc*, **137**, 553–597, doi:10.1002/qj.828.

Glaccum, W., R. L. Lucke, R. M. Bevilacqua, E. P. Shettle, J. S. Hornstein, D. T. Chen, J. D. Lumpe, S. S. Krigman, D. J. Debrestian, M. D. Fromm, F. Dalaudier, E. Chassefière, C. Deniel, C. E. Randall, D. W. Rusch, J. J. Olivero, C. Brogniez, J. Lenoble, and R. Kremer, 1996: The Polar Ozone and Aerosol Measurement instrument. *J. Geophys. Res.*, **101**, 14479–14487, doi:10.1029/96JD00576.

Harada, Y., A. Goto, H. Hasegawa, N. Fujikawa, H. Naoe, and T. Hirooka, 2010: A Major Stratospheric Sudden Warming Event in January 2009. *J. Atmos. Sci.*, **67**, 2052–2069, doi:10.1175/2009JAS3320.1.

Hardiman, S. C., N. Butchart, A. J. Charlton-Perez, T. A. Shaw, H. Akiyoshi, A. Baumgaertner, S. Bekki, P. Braesicke, M. Chipperfield, M. Dameris, R. R. Garcia, M. Michou, S. Pawson, E. Rozanov, and K. Shibata, 2011: Improved predictability of the troposphere using stratospheric final warmings. *J. Geophys. Res.*, **116**, D18113, doi:10.1029/2011JD015914.

Hartmann, D. L., L. E. Heidt, M. Loewenstein, J. R. Podelske, J. Vedder, W. L. Starr, and S. E. Strahan, 1989: Transport into the South Polar vortex in early spring. *J. Geophys. Res.*, **94**, 16779–16796, doi:10.1029/JD094iD14p16779.

Haynes, P., and E. Shuckburgh, 2000: Effective diffusivity as a diagnostic of atmospheric transport 1. Stratosphere. *J. Geophys. Res.*, **105**, 22777–22794, doi:10.1029/2000JD900093.

Hu, J., R. Ren, and H. Xu, 2014: Occurrence of winter stratospheric sudden warming events and the seasonal timing of spring stratospheric final warming. *J. Atmos. Sci.*, **71**, 2319–2334, doi:10.1175/JAS-D-13-0349.1.

Karpetchko, A., E. Kyrö, and B. M. Knudsen, 2005: Arctic and Antarctic polar vortices 1957–2002 as seen from the ERA-40 reanalyses. *J. Geophys. Res.*, **110**, D21109, doi:10.1029/2005JD006113.

Lait, L. R., 1994: An alternative form for potential vorticity. *J. Atmos. Sci.*, **51**, 1754–1759, doi:10.1175/1520-0469(1994)051<1754:AAFFPV>2.0.CO;2.

Langematz, U., and M. Kunze, 2006: An update on dynamical changes in the Arctic and Antarctic stratospheric polar vortices. Clim. Dyn., **27**, 647-660, doi:10.1007/s00382-006-0156-2.

Lucke, R. L., D. R. Korwan, R. M. Bevilacqua, J. S. Hornstein, E. P. Shettle, D. T. Chen, M. Daehler, J. D. Lumpe, M. D. Fromm, D. Debrestian, B. Neff, M. Squire, G. König-Langlo, and J. Davies, 1999: The Polar Ozone and Aerosol Measurement (POAM) III instrument and early validation results. *J. Geophys. Res.*, **104**, 18785–18799, doi:10.1029/1999JD900235.

Manney, G. L., R. W. Zurek, M. E. Gelman, A. J. Miller, and R. Nagatani, 1994: The anomalous Arctic lower stratospheric polar vortex of 1992–1993. *Geophys. Res. Lett.*, **21**, 2405–2408, doi:10.1029/94GL02368.

Manney, G. L., and J. L. Sabutis, 2000: Development of the polar vortex in the 1999-2000 Arctic winter stratosphere. *Geophys. Res. Lett.*, **27**, 2589–2592, doi:10.1029/2000GL011703.

Marlton, G., A. Charlton-Perez, G. Harrison, I. Polichtchouk, A. Hauchecorne, P. Keckhut, R. Wing, T. Leblanc, and W. Steinbrecht, 2021: Using a network of temperature lidars to identify temperature biases in the upper stratosphere in ECMWF reanalyses. *Atmos. Chem. Phys.*, **21**, 6079–6092, doi:10.5194/acp-21-6079-2021.

Nakamura, N., and J. Ma, 1997: Modified Lagrangian-mean diagnostics of the stratospheric polar vortices: 2. Nitrous oxide and seasonal barrier migration in the cryogenic limb array etalon spectrometer and SKYHI general circulation model. *J. Geophys. Res.*, **102**, 25721–25735, doi:10.1029/97JD02153.

Nash, E. R., P. A. Newman, J. E. Rosenfield, and M. R. Schoeberl, 1996: An objective determination of the polar vortex using Ertel's potential vorticity. *J. Geophys. Res.*, **101**, 9471–9478, doi:10.1029/96JD00066.

Nath, D., W. Chen, C. Zelin, A. I. Pogoreltsev, and K. Wei, 2016: Dynamics of 2013 Sudden Stratospheric Warming event and its impact on cold weather over Eurasia: Role of planetary wave reflection. *Sci. Rep.*, **6**, 24174, doi:10.1038/srep24174.

Neu, J. L., and L. C. Sparling, 2003: Plumb, R.A. Variability of the subtropical “edges” in the stratosphere. *J. Geophys. Res.*, **108**, 4482, doi:10.1029/2002JD002706.

Polvani, L. M., D. W. Waugh, and R. A. Plumb, 1995: On the subtropical edge of the stratospheric surf zone. *J. Atmos. Sci.*, **52**, 1288–1309, doi:10.1175/1520-0469(1995)052<1288:OTSEOT>2.0.CO;2.

Sasano, Y., M. Suzuki, T. Yokota, and H. Kanzawa, 1999: Improved Limb Atmospheric Spectrometer (ILAS) for stratospheric ozone layer measurements by solar occultation technique. *Geophys. Res. Lett.*, **26**, 197–200, doi:10.1029/1998GL900276.

Schoeberl, M. R., L. R. Lait, P. A. Newman, and J. E. Rosenfield, 1992: The structure of the polar vortex. *J. Geophys. Res.*, **97**, 7859–7882, doi:10.1029/91JD02168.

Solomon, S., 1999: Stratospheric ozone depletion: A review of concepts and history. *Rev. Geophys.*, **37**, 275–316, doi:10.1029/1999RG900008.

Waugh, D. W., and L. M. Polvani, 2010: Stratospheric polar vortices. *The Stratosphere: Dynamics, Transport, and Chemistry, Geophysical Monograph Series*. Wiley, Hoboken, NJ, USA,; Volume 190, pp. 43–57, doi:10.1002/9781118666630.ch3.

Waugh, D. W., and W. J. Randel, 1999: Climatology of Arctic and Antarctic polar vortices using elliptical diagnostics. *J. Atmos. Sci.*, **56**, 1594–1613, doi:10.1175/1520-0469(1999)056<1594:COAAAP>2.0.CO;2.

Waugh, D. W., W. J. Randel, S. Pawson, P. A. Newman, and E. R. Nash, 1999: Persistence of the lower stratospheric polar vortices. *J. Geophys. Res.*, **104**, 27191–27201, doi:10.1029/1999JD900795.

Yokota, T., H. Nakajima, T. Sugita, H. Tsubaki, Y. Itou, M. Kaji, M. Suzuki, H. Kanzawa, J. H. Park, and Y. Sasano, 2002: Improved Limb Atmospheric Spectrometer (ILAS) data retrieval algorithm for Version 5.20 gas profile products. *J. Geophys. Res.*, **107**, 8216, doi:10.1029/2001JD000628.

Zambri, B., S. Solomon, D. W. J. Thompson, and Q. Fu, 2021: Emergence of Southern Hemisphere stratospheric circulation changes in response to ozone recovery. *Nat. Geosci.*, **14**, 638–644, doi:10.1038/s41561-021-00803-3.

List of Figures

Fig. 1 Isolines of MPV (contours, PVU) and its meridional gradient (red shading) over EL and time, on the 450 K isentropic surface in the NH for 1996–1997. The blue contour represents the average wind speed (m s^{-1}) along the MPV isoline. Black squares indicate the edge of the polar vortex. Red vertical lines A, B, and C denote 10 March, 10 May, and 20 May, respectively.

Fig. 2 MPV gradient (red line) and wind speed (blue) along MPV isolines versus EL on the 450 K surface on (a) 10 March, 1997, (b) 10 May, 1997, and (c) 20 May, 1997, and in the right panel their corresponding MPV fields (d), (e), and (f) for the same dates, respectively. Location of the vortex edge on each day is marked by a dotted line in the left panel and a thick black solid contour in the right panel.

Fig. 3 On the 450 K surface: (a) Black squares and line denote the values of MPV at the vortex edge and 80°N in EL, respectively. Horizontal dashed line represents 18.6 PVU, and green vertical lines represent the 3-month winter period; (b) Maximum wind speed along MPV isolines. Horizontal dashed line represents 15.2 m s^{-1}; (c) Zonal wind speed for which the contour encloses the area equivalent to 75°. Horizontal dashed line indicates 25 m s^{-1}.

Fig. 4 (a) Isolines of MPV (contours, PVU) over EL and time, on the 1260 K isentropic surface in the NH for 1996–1997. Green and blue contours represent 18.9 and 14.4 PVU, respectively. Black squares indicate the edge of the polar vortex. Red vertical lines A, B, C, and D denote 15 January, 10 February, 25 March, and 15 April, 1997, respectively. (b) Black squares show the MPV at the vortex edge. The two horizontal dashed lines represent 18.9 PVU and 14.4 PVU, respectively. Green vertical lines represent the 3-month winter period. Blue vertical lines represent the period from 18 February through to 10 April.

Fig. 5 Same as in Fig. 2, but on the 1260 K surface for (a) 15 January, (b) 10 February, (c) 25 March, and (d) 15 April, all in 1997, and (e)–(h) are their corresponding MPV fields. Location of the subtropical edge is marked by a dotted line in (d) and dotted contour in (h).

Fig. 6 Isolines of MPV (contours, PVU) and its meridional gradient (red shading) in EL (10°S–80°N) and time on the 1260 K isentropic surface in the NH for 1996–1997. The blue contour represents the average wind speed (m s^{-1}) along the MPV isoline. Black squares indicate the edge of the polar vortex.

Fig. 7 Changes in time of (a) EL at the vortex edge, (b) MPV, (c) average wind speed along the MPV isoline at the vortex edge on the 1260 K surface, and (d) normalized changes of EL (green line), MPV (red), wind speed (blue), and their average (black) at the vortex edge.

Fig. 8 Comparison of polar vortex breakup dates in the NH on 510 K isentropic surfaces for the period 1979–2018 using the “PV and U”, “U area”, “PV area”, and “edge-change” criteria. Red diamonds denote the years of 2009 and 2013.

Fig. 9 Isolines of MPV (contours, PVU) and its meridional gradient (red shading) in EL (10°S–80°N) and time on the 510 K isentropic surface (upper panels) and normalized changes of EL, MPV, wind speed, and their average in the NH (lower panels) for (a) 2008–2009 and (b) 2012–2013. The blue contour represents the average wind speed (m s^{-1}) along the MPV isoline. Black squares indicate the edge of the polar vortex.

Fig. 10 The dates of formation and breakup of the NH and the SH polar vortex (orange line) and their average (thick black line) from 430 K to 1260 K for the period 1979–2018.

Fig. 11 Black solid lines denote the vortex breakup dates determined by the “edge-change” method at (a) 1260 K in NH, (b) 1260 K in SH, (c) 510 K in NH, and (d)

510 K in SH for the period of 1979–2018. Red solid and dotted lines in (b) and (d) are the linear trends for 1979–2000 and 2000–2018, respectively. The red solid line is statistically significant at the 95% confidence level (p=0.018).

Fig. 12 Zonal-mean zonal wind (m s^{-1}) from 430 K to 1260 K averaged from 60°N to 80°N for the period of 1992–2005. Red circles and green diamonds denote the dates of the vortex breakup obtained by the "edge-change" method and the SFW defined by the 10 m s^{-1} threshold, respectively. Yellow squares denote the SFW defined by the 5 m s^{-1} threshold.

Fig. 13 CH_4 and O_3 mixing ratios observed by ILAS in EL and time on the 1260 K, 800 K, and 450 K isentropic surfaces in the NH from 1 November, 1996, to 30 June, 1997. The black square denotes the location of the vortex edge each day, and the vertical line represents the date of the polar vortex breakup using the “edge-change” method.

Fig. 14 Standard deviation of the mixing ratios of (a) CH_4, (b) N_2O, (c) H_2O, and (d) O_3 following the latitude circle from the ILAS observations for 1 November, 1996, to 30 June, 1997. Gray isolines represent the potential temperature, and the red solid circle denotes the date of the polar vortex breakup on each isentropic surface using the “edge-change” method.

Fig. 15 The standard deviation of the O_3 mixing ratio (denoted by color shading) following the latitude circle from the POAM II (October 1993–November 1996), ILAS (November 1996–June 1997), and POAM III (April 1998–November 2005) observations, and the daily maximum MPV (10^{-6} K m^2 kg^{-1} s^{-1}; denoted by contours) on each isentropic surface in the NH for the period 1992–2005. Red solid diamonds and circles denote the dates of the formation and breakup of the polar vortex, respectively. In the lower part of each panel, the latitudes of the POAM II, ILAS, and POAM III observations are represented by blue, yellow, and red lines, respectively.

Fig. 16 Same as in Fig. 15, but for the SH. Contour lines represent the daily minimum MPV on each isentropic surface.

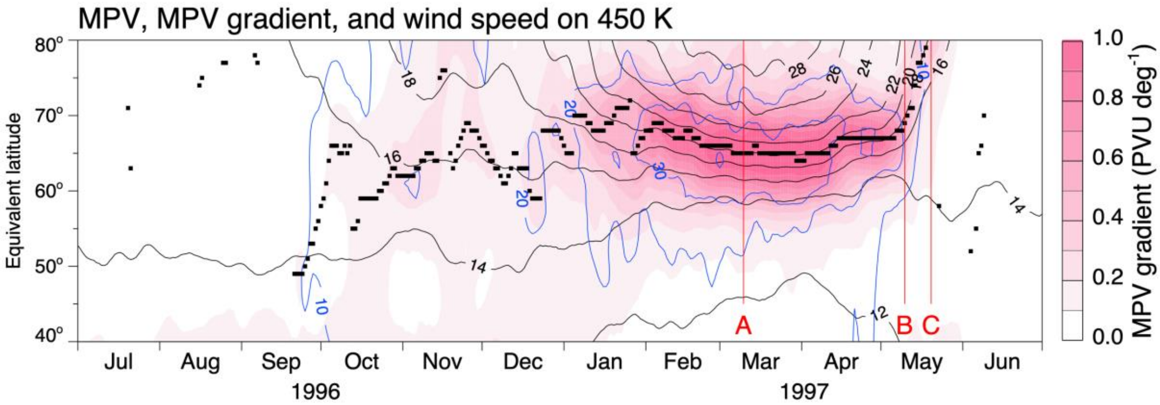

Fig. 1 Isolines of MPV (contours, PVU) and its meridional gradient (red shading) over EL and time, on the 450 K isentropic surface in the NH for 1996–1997. The blue contour represents the average wind speed (m s^{-1}) along the MPV isoline. Black squares indicate the edge of the polar vortex. Red vertical lines A, B, and C denote 10 March, 10 May, and 20 May, respectively.

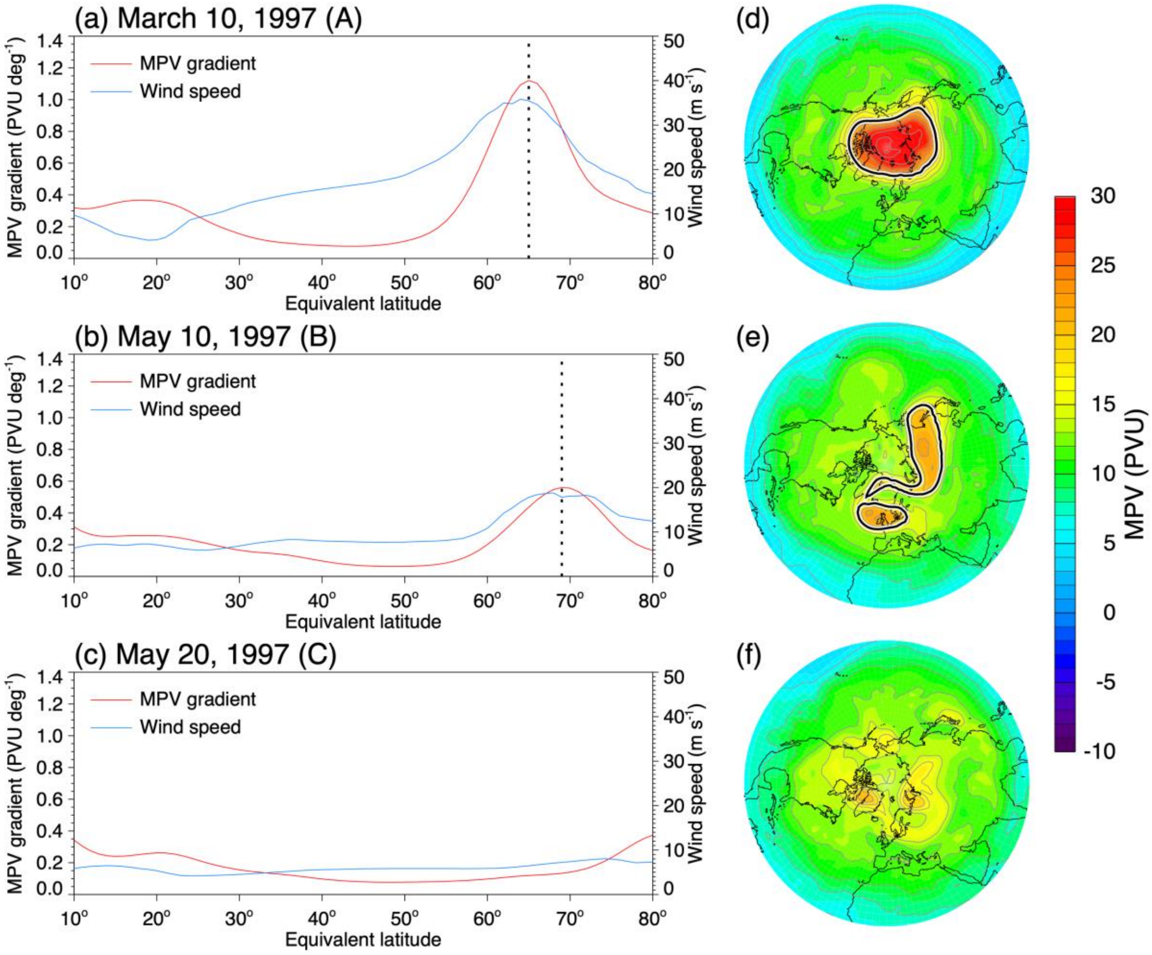

Fig. 2 MPV gradient (red line) and wind speed (blue) along MPV isolines versus EL on the 450 K surface on (a) 10 March, 1997, (b) 10 May, 1997, and (c) 20 May, 1997, and in the right panel their corresponding MPV fields (d), (e), and (f) for the same dates, respectively. Location of the vortex edge on each day is marked by a dotted line in the left panel and a thick black solid contour in the right panel.

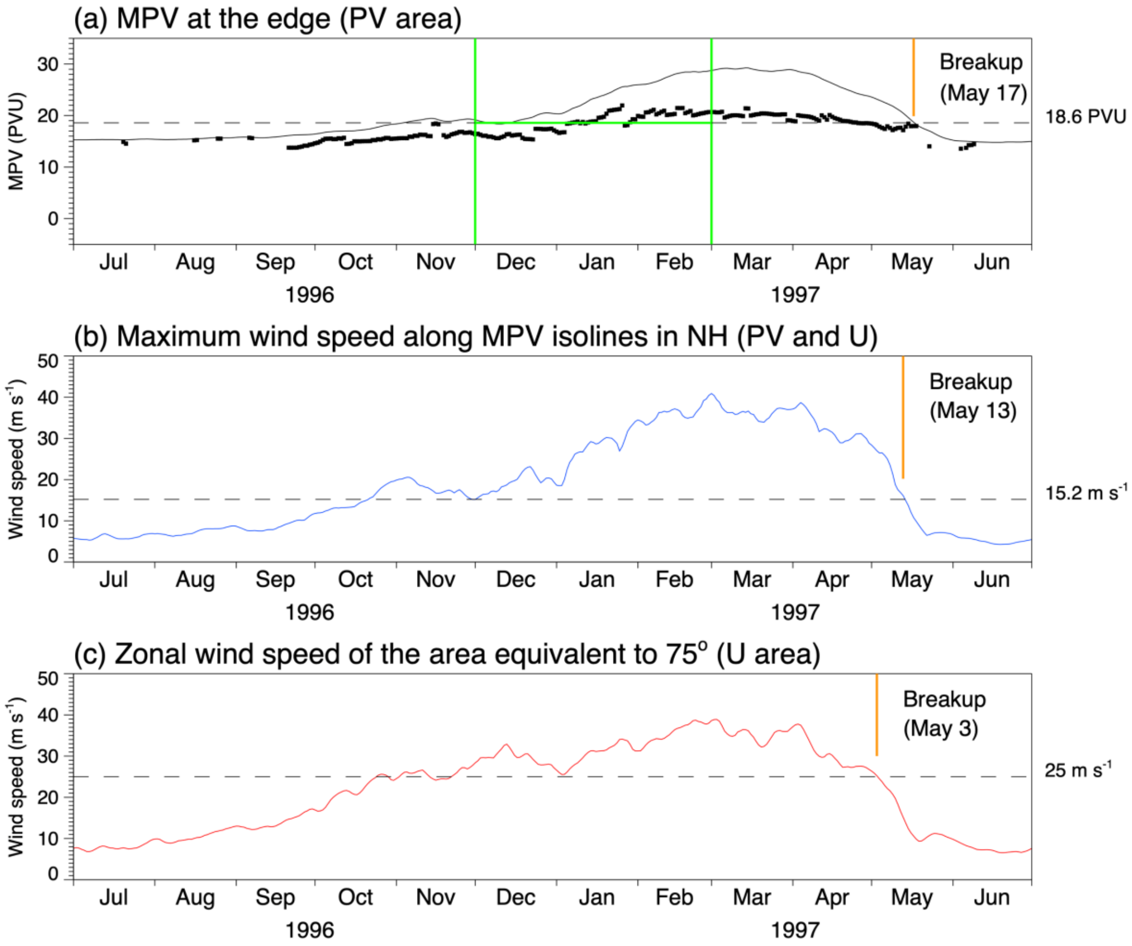

Fig. 3 On the 450 K surface: (a) Black squares and line denote the values of MPV at the vortex edge and 80°N in EL, respectively. Horizontal dashed line represents 18.6 PVU, and green vertical lines represent the 3-month winter period; (b) Maximum wind speed along MPV isolines. Horizontal dashed line represents 15.2 m s^{-1}; (c) Zonal wind speed for which the contour encloses the area equivalent to 75°. Horizontal dashed line indicates 25 m s^{-1}.

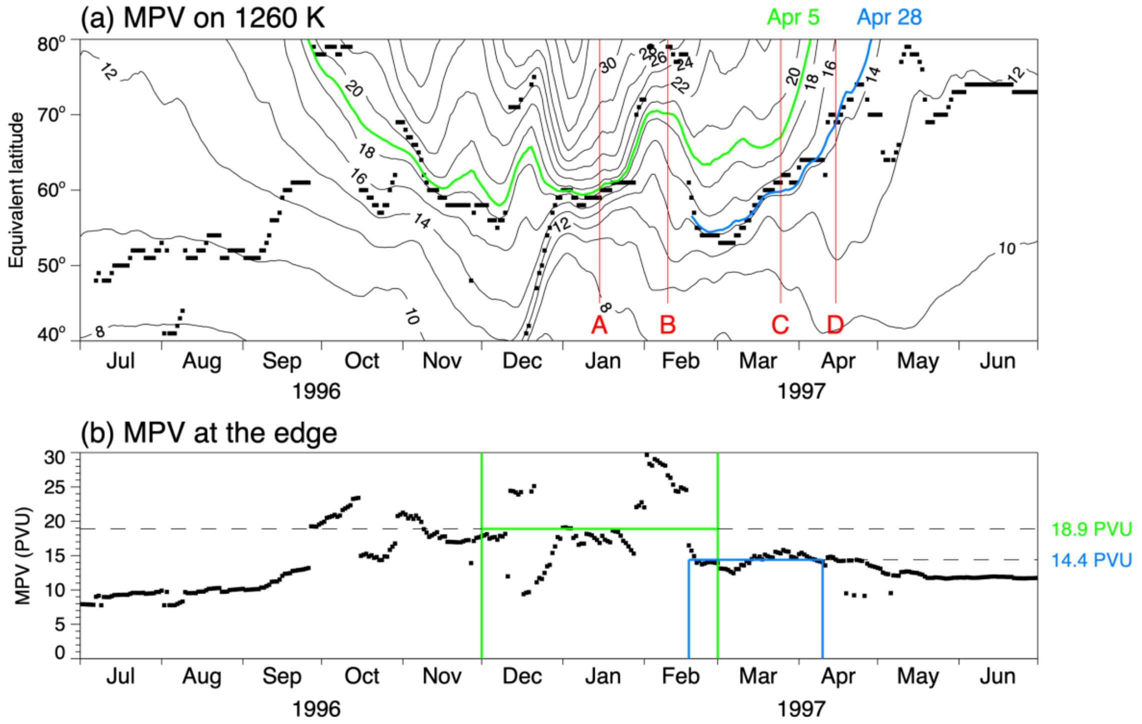

Fig. 4 (a) Isolines of MPV (contours, PVU) over EL and time, on the 1260 K isentropic surface in the NH for 1996–1997. Green and blue contours represent 18.9 and 14.4 PVU, respectively. Black squares indicate the edge of the polar vortex. Red vertical lines A, B, C, and D denote 15 January, 10 February, 25 March, and 15 April, 1997, respectively. (b) Black squares show the MPV at the vortex edge. The two horizontal dashed lines represent 18.9 PVU and 14.4 PVU, respectively. Green vertical lines represent the 3-month winter period. Blue vertical lines represent the period from 18 February through to 10 April.

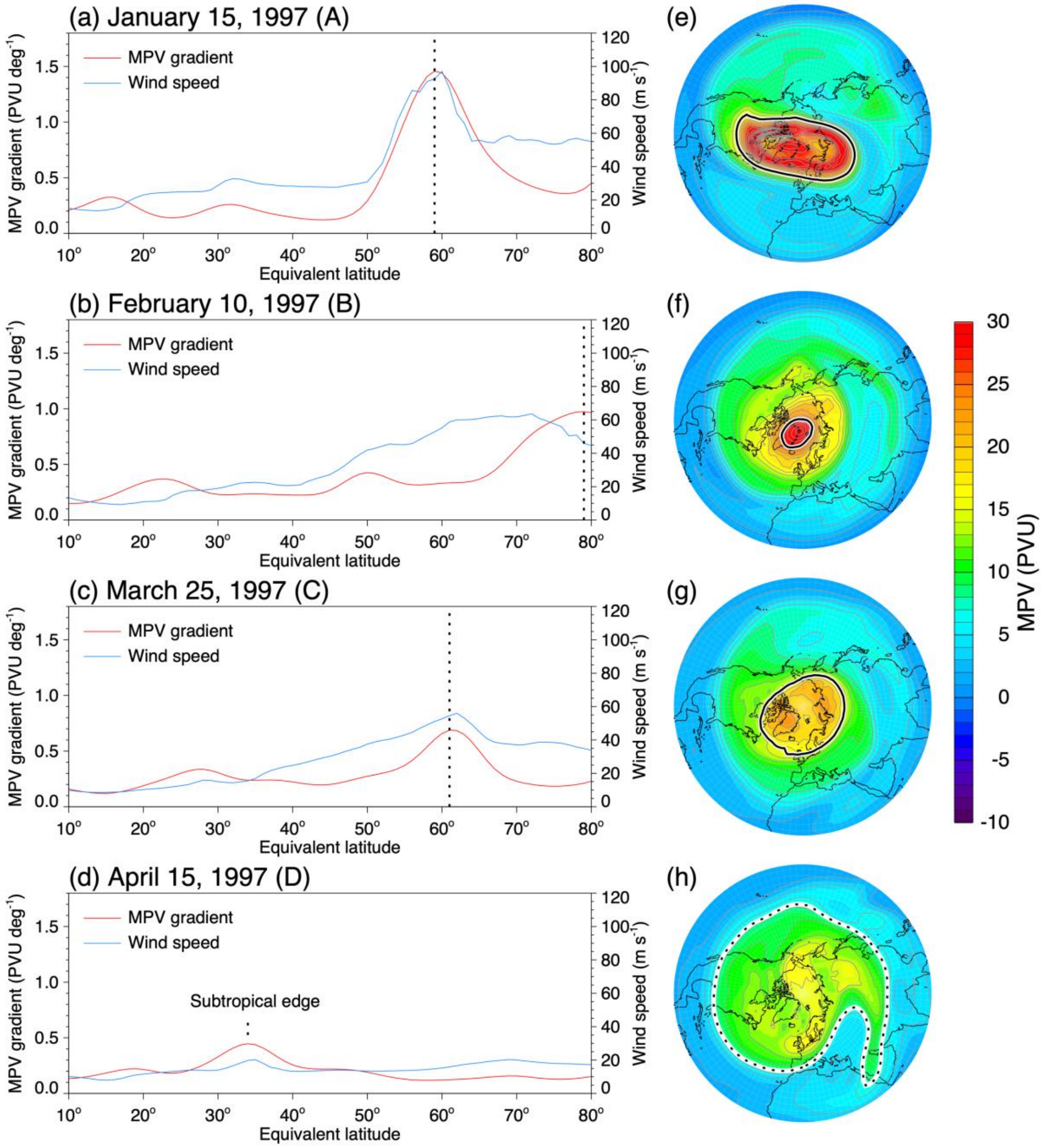

Fig. 5 Same as in Fig. 2, but on the 1260 K surface for (a) 15 January, (b) 10 February, (c) 25 March, and (d) 15 April, all in 1997, and (e)–(h) are their corresponding MPV fields. Location of the subtropical edge is marked by a dotted line in (d) and dotted contour in (h).

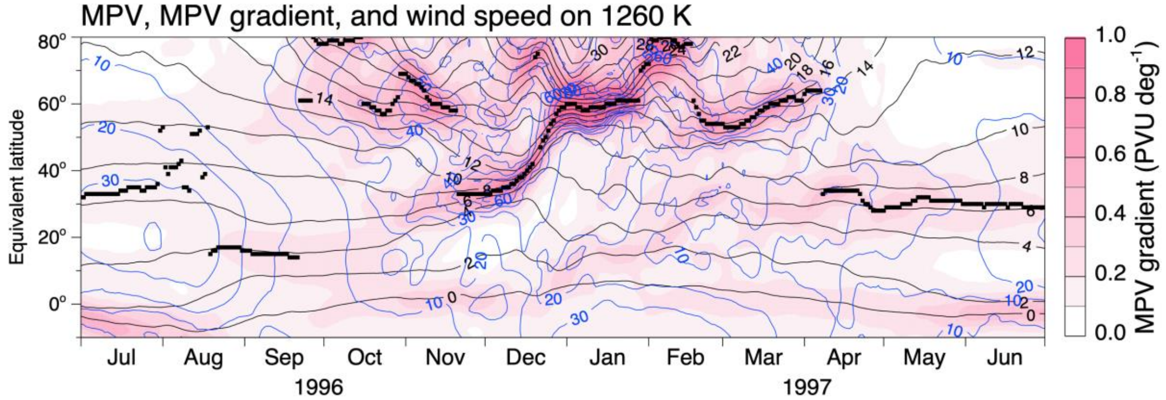

Fig. 6 Isolines of MPV (contours, PVU) and its meridional gradient (red shading) in EL (10°S–80°N) and time on the 1260 K isentropic surface in the NH for 1996–1997. The blue contour represents the average wind speed (m s^{-1}) along the MPV isoline. Black squares indicate the edge of the polar vortex.

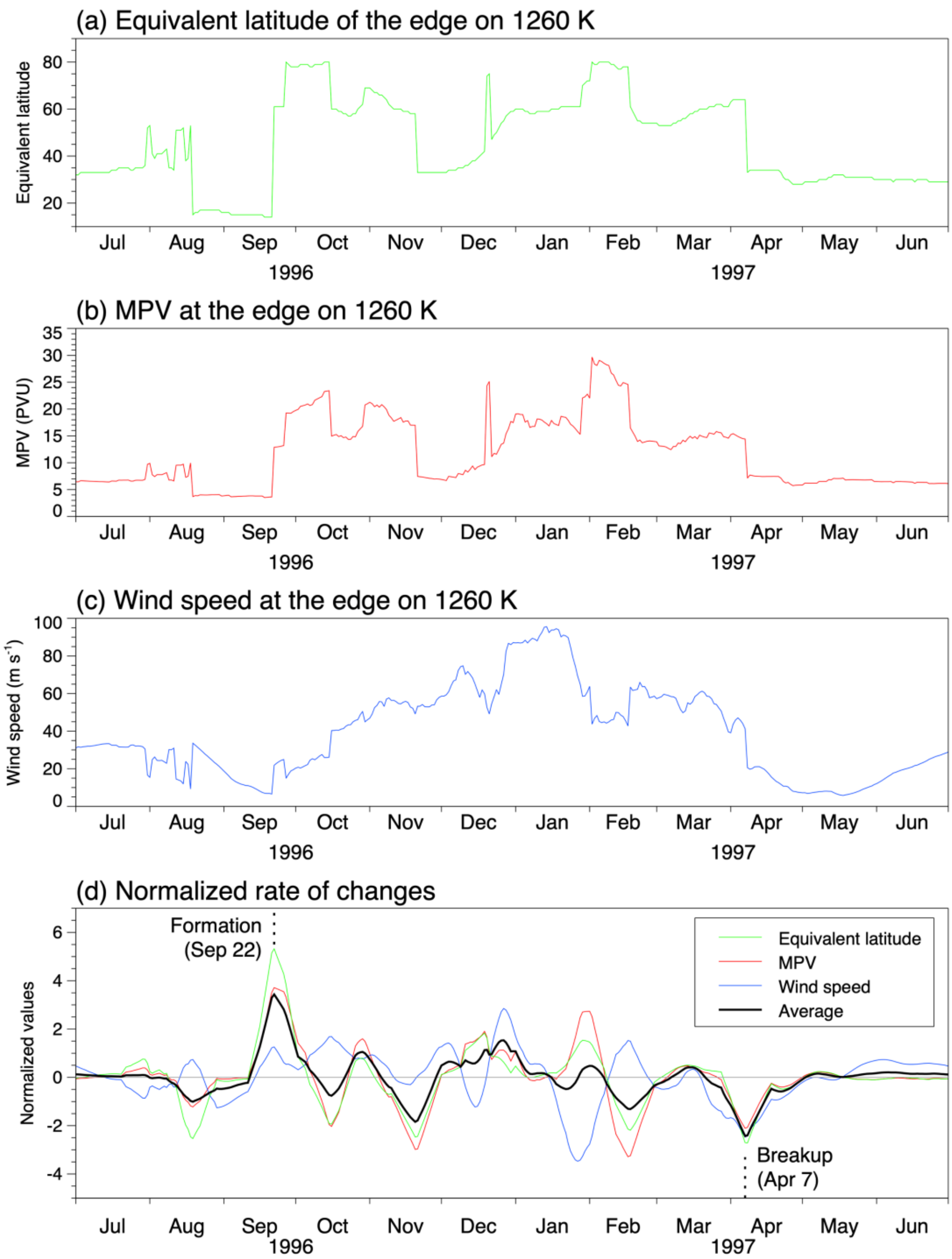

Fig. 7 Changes in time of (a) EL at the vortex edge, (b) MPV, (c) average wind speed along the MPV isoline at the vortex edge on the 1260 K surface, and (d) normalized changes of EL (green line), MPV (red), wind speed (blue), and their average (black) at the vortex edge.

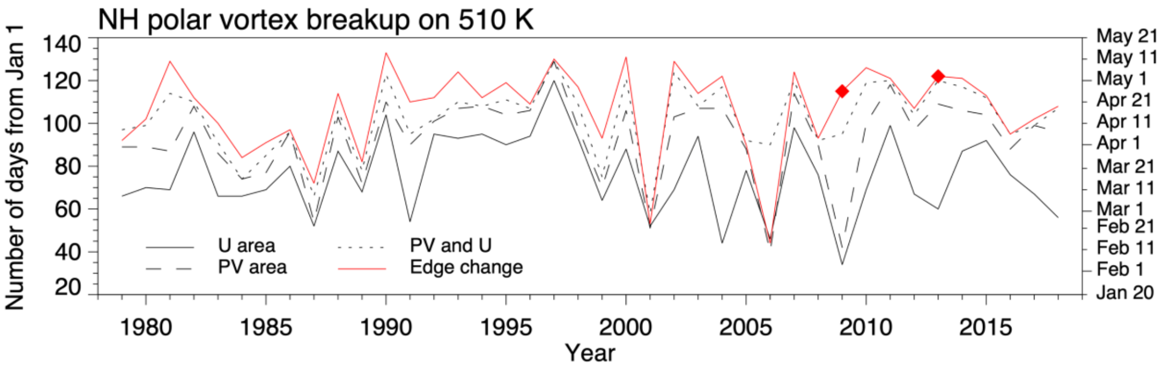

Fig. 8 Comparison of polar vortex breakup dates in the NH on 510 K isentropic surfaces for the period 1979–2018 using the “PV and U”, “U area”, “PV area”, and “edge-change” criteria. Red diamonds denote the years of 2009 and 2013.

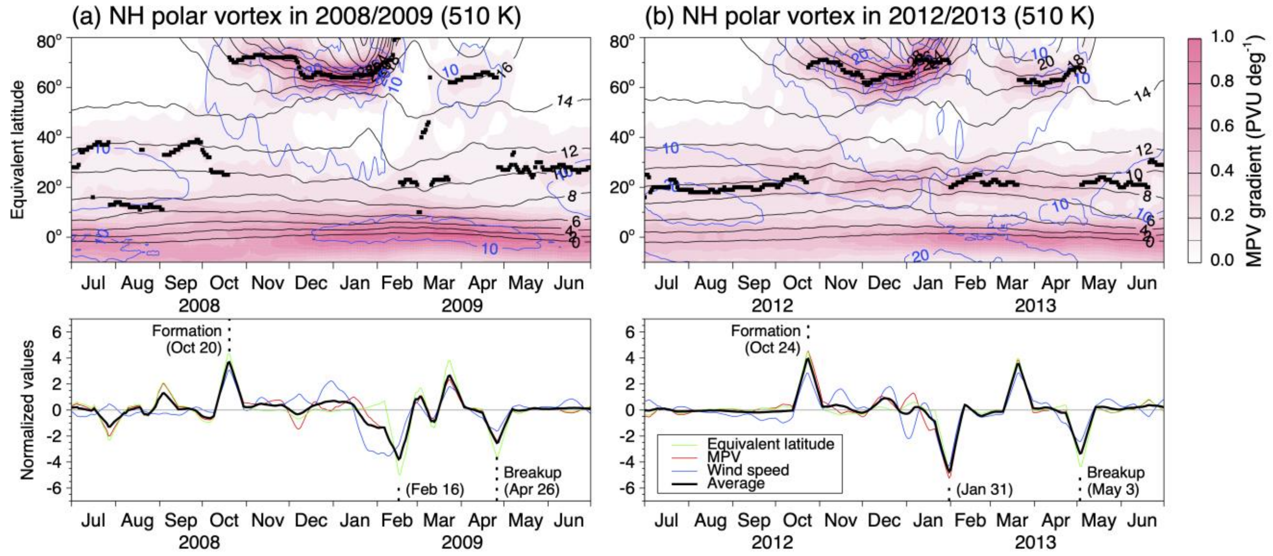

Fig. 9 Isolines of MPV (contours, PVU) and its meridional gradient (red shading) in EL (10°S–80°N) and time on the 510 K isentropic surface (upper panels) and normalized changes of EL, MPV, wind speed, and the "edge change" metric in the NH (lower panels) for (a) 2008–2009 and (b) 2012–2013. The blue contour represents the average wind speed (m s^{-1}) along the MPV isoline. Black squares indicate the edge of the polar vortex.

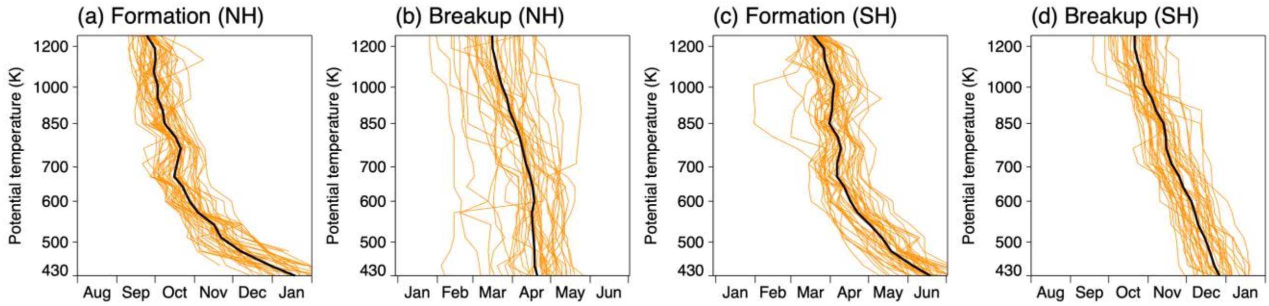

Fig. 10 The dates of formation and breakup of the NH and the SH polar vortex (orange line) and their average (thick black line) from 430 K to 1260 K for the period 1979–2018.

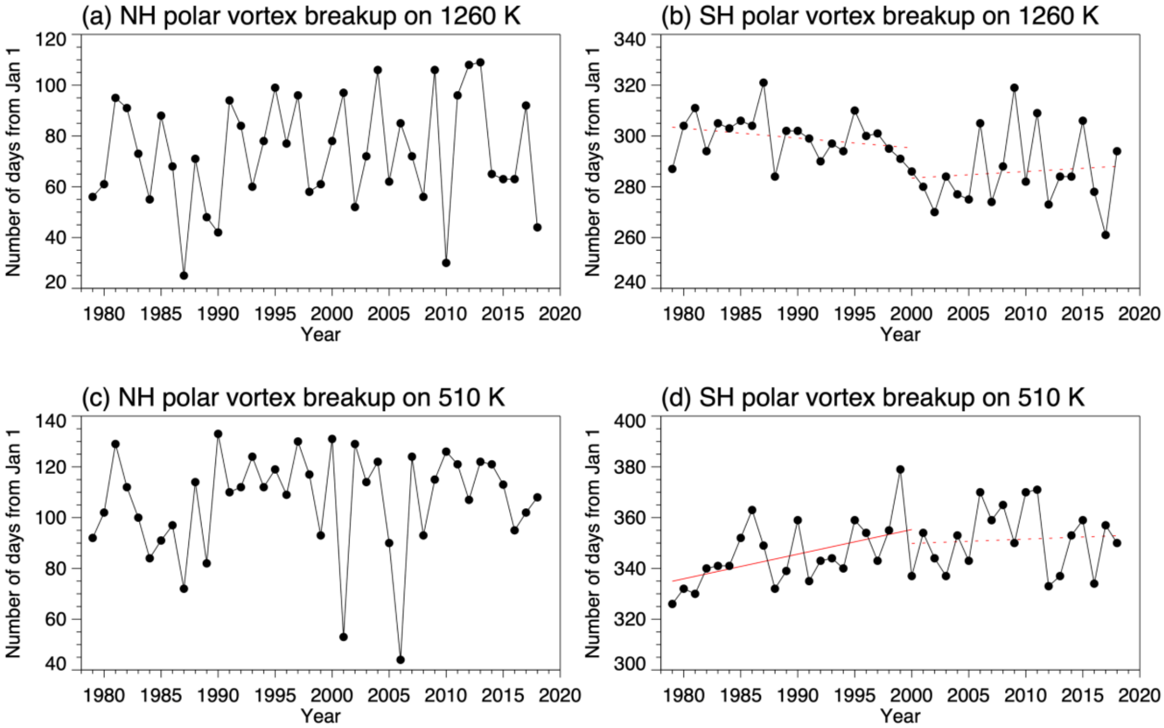

Fig. 11 Black solid lines denote the vortex breakup dates determined by the "edge-change" method at (a) 1260 K in NH, (b) 1260 K in SH, (c) 510 K in NH, and (d) 510 K in SH for the period of 1979–2018. Red solid and dotted lines in (b) and (d) are the linear trends for 1979–2000 and 2000–2018, respectively. The red solid line is statistically significant at the 95% confidence level (p=0.018).

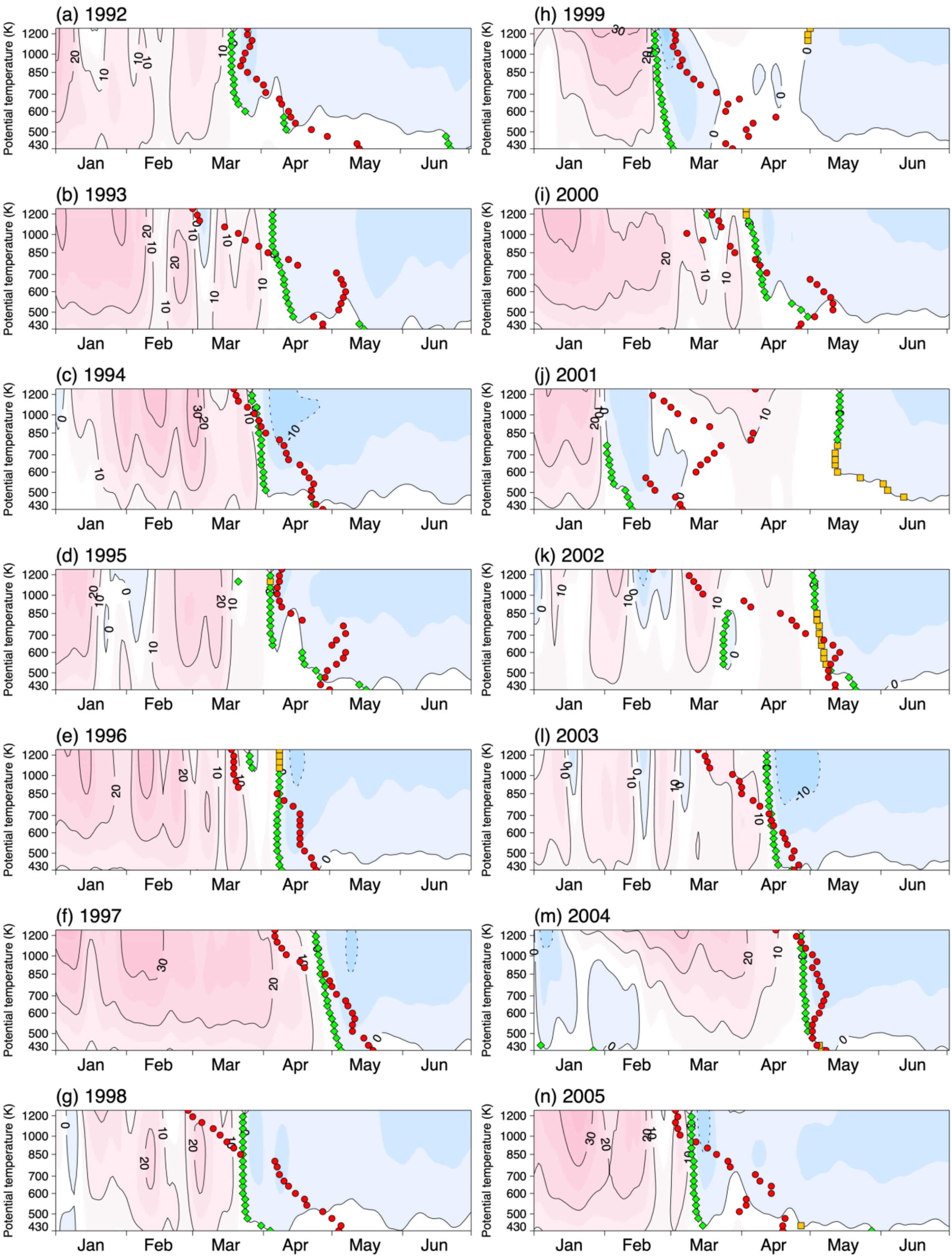

Fig. 12 Zonal-mean zonal wind (m s^{-1}) from 430 K to 1260 K averaged from 60°N to 80°N for the period of 1992–2005. Red circles and green diamonds denote the dates of the

vortex breakup obtained by the "edge-change" method and the SFW defined by the 10 m s^{-1} threshold, respectively. Yellow squares denote the SFW defined by the 5 m s^{-1} threshold.

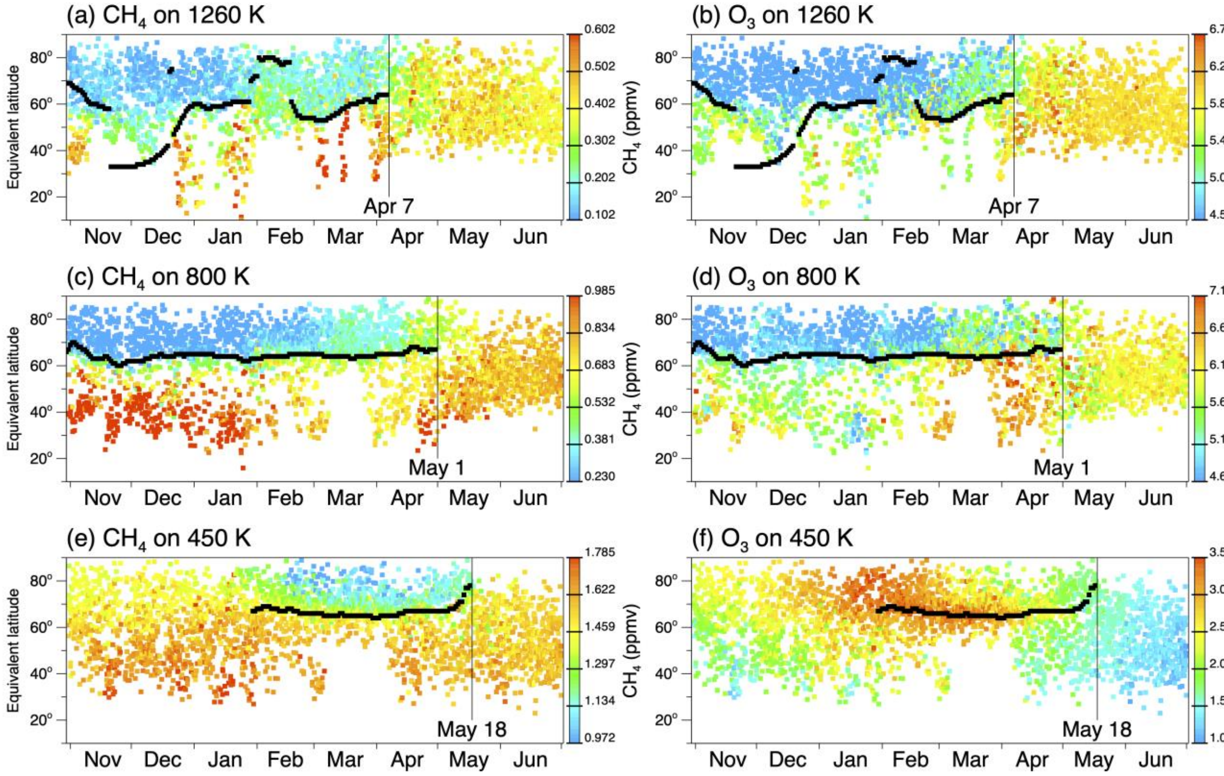

Fig. 13 CH_4 and O_3 mixing ratios observed by ILAS in EL and time on the 1260 K, 800 K, and 450 K isentropic surfaces in the NH from 1 November, 1996, to 30 June, 1997. The black square denotes the location of the vortex edge each day, and the vertical line represents the date of the polar vortex breakup using the “edge-change” method.

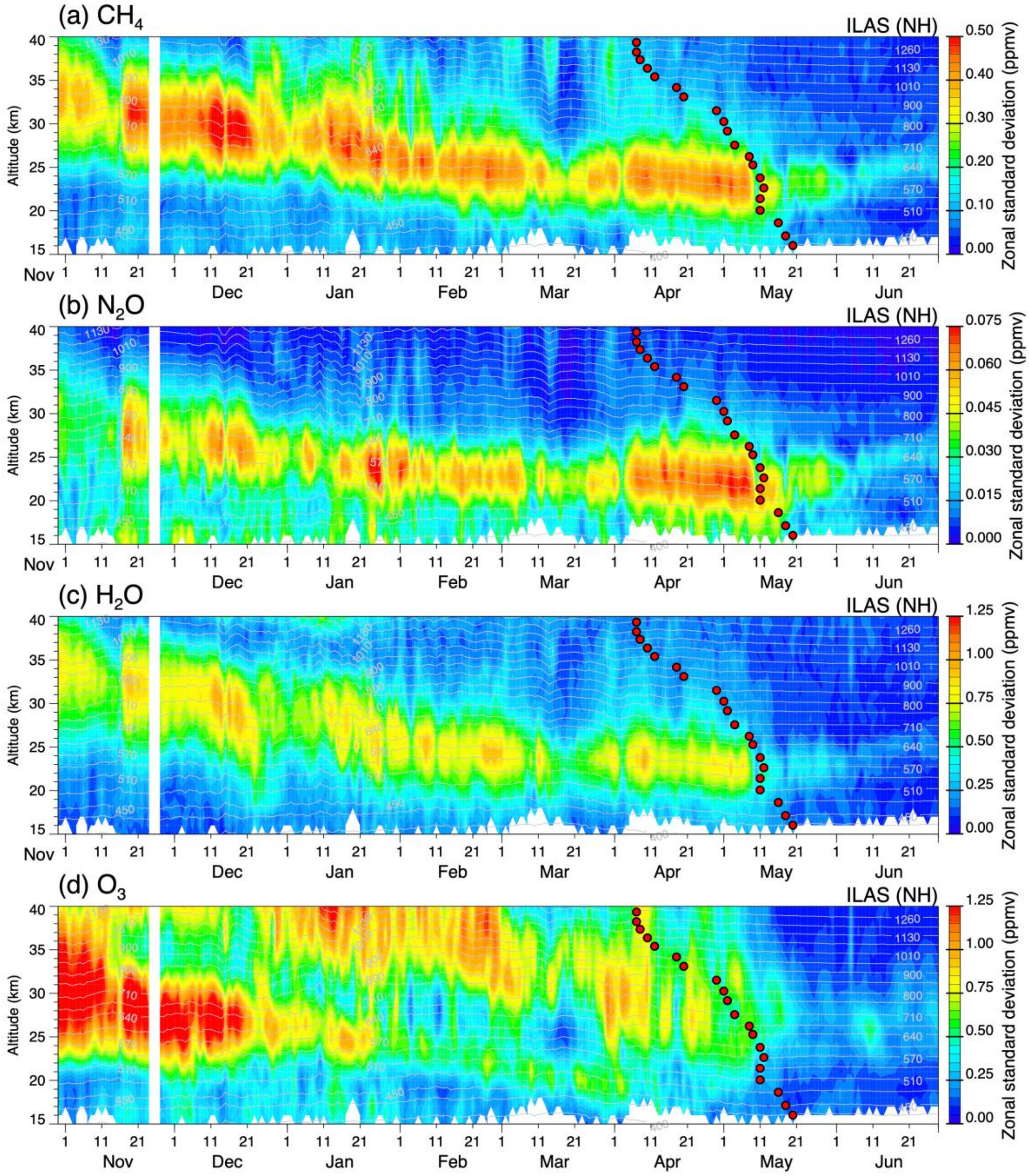

Fig. 14 Standard deviation of the mixing ratios of (a) CH_4, (b) N_2O, (c) H_2O, and (d) O_3 following the latitude circle from the ILAS observations for 1 November, 1996, to 30 June, 1997. Gray isolines represent the potential temperature, and the red solid circle denotes the date of the polar vortex breakup on each isentropic surface using the “edge-change” method.

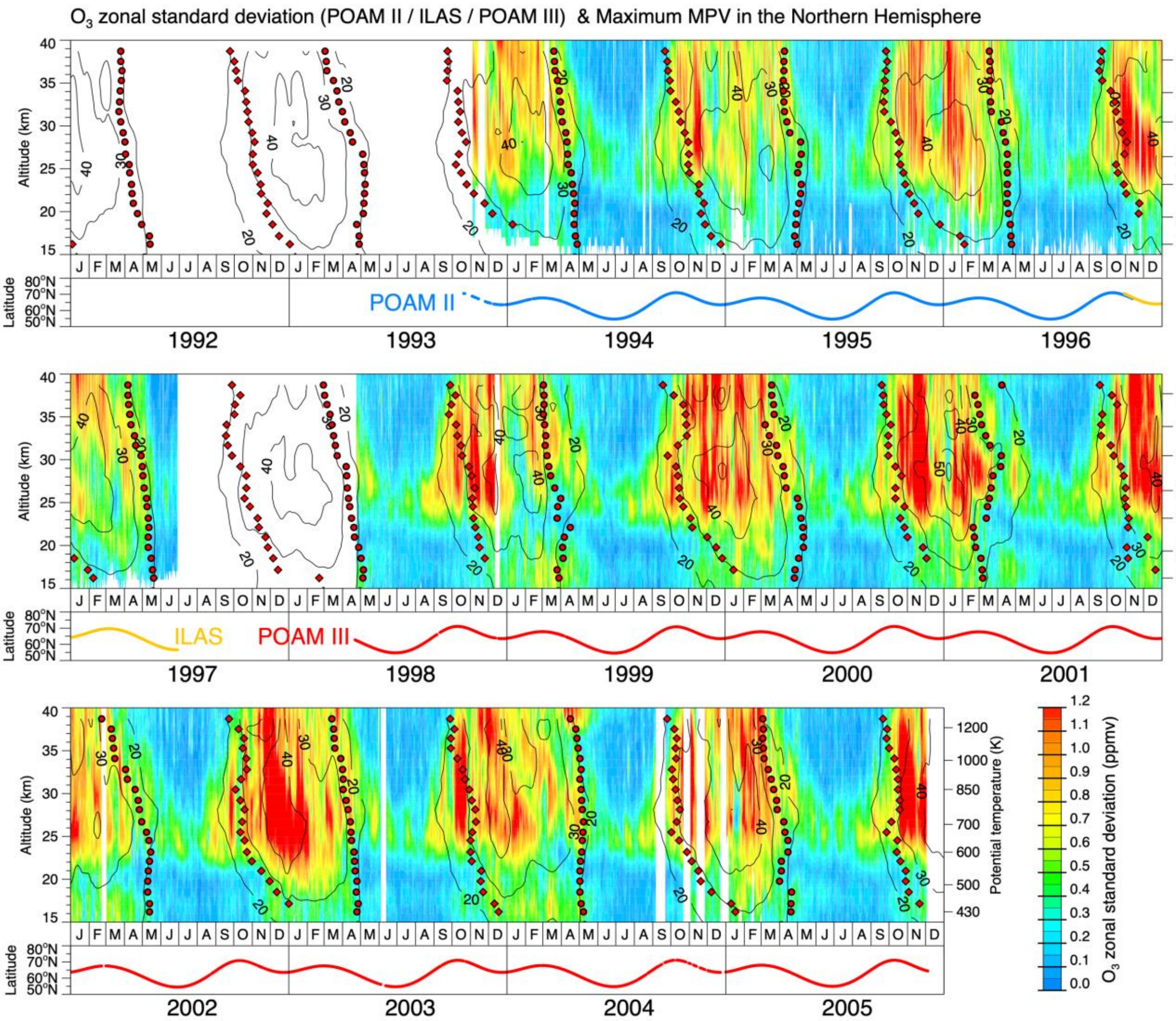

Fig. 15 The standard deviation of the O_3 mixing ratio (denoted by color shading) following the latitude circle from the POAM II (October 1993–November 1996), ILAS (November 1996–June 1997), and POAM III (April 1998–November 2005) observations, and the daily maximum MPV (10^{-6} K m^2 kg^{-1} s^{-1}; denoted by contours) on each isentropic surface in the NH for the period 1992–2005. Red solid diamonds and circles denote the dates of the formation and breakup of the polar vortex, respectively. In the lower part of each panel, the latitudes of the POAM II, ILAS, and POAM III observations are represented by blue, yellow, and red lines, respectively.

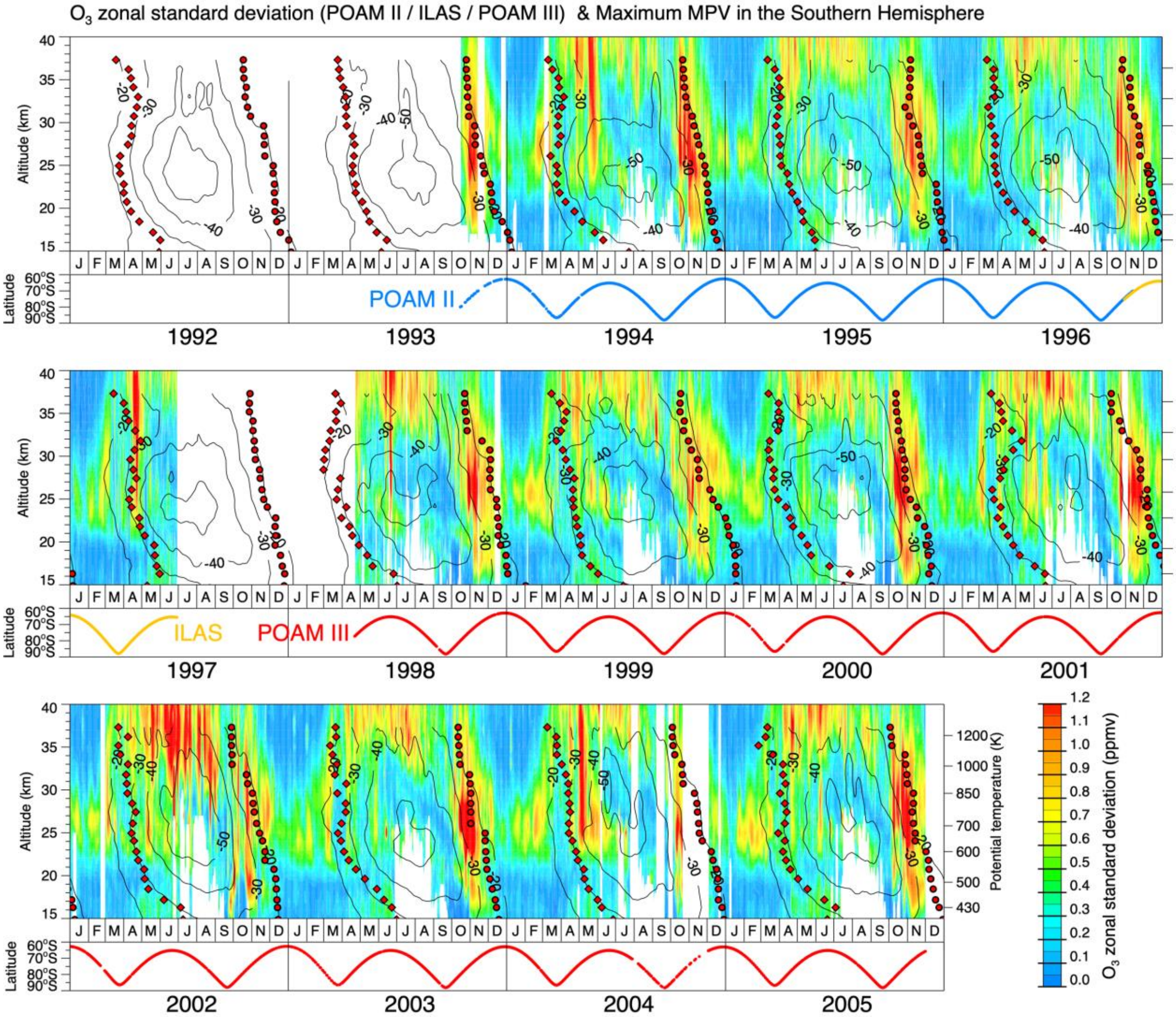

Fig. 16 Same as in Fig. 15, but for the SH. Contour lines represent the daily minimum MPV on each isentropic surface.